Generation of dc voltages by a magnetic multilayer undergoing ferromagnetic resonance

L. Berger
Department of Physics, Carnegie Mellon University, Pittsburgh, Pennsylvania 15213
(Received 14 October 1998)

We predict that a dc voltage V appears across a magnetic multilayer undergoing ferromagnetic resonance. The voltage exists along a direction perpendicular to the layer plane. This is the magnetic analog of a photovoltaic cell. We calculate the rate of spin flip of conduction-electron spins, induced by the precession of the magnetization. Also, we solve the Valet-Fert spin-diffusion equation in the various layers. The dc voltage V is obtained by combining these two equations. For sufficiently large precession amplitude, V converges toward a fixed value of order $\simeq \hbar\omega/e \simeq 10\,\mu$V, where ω is the angular frequency of precession and e the electron charge. [S0163-1829(99)04517-8]

I. INTRODUCTION

Recently, we predicted[1–3] that a dc current crossing an interface between the normal and ferromagnetic layer, in metallic multilayers, would induce a precession of the magnetization in the ferromagnetic layer. The presence of the sharp interface causes[1] a local increase of the magnon-electron interaction. Also, the interface acts as a source of momentum, helping the conduction electrons to jump across the momentum gap between spin-up and spin-down Fermi surfaces as they emit spin waves, i.e., as they generate the precession. We call this device a SWASER. Slonczewski has proposed[4] a similar current-induced spin precession, as well as a switching of the magnetization between two different static directions. Recently, Tsoi *et al.*[5] have obtained experimental evidence of such spin precession, in a Cu/Co multilayer traversed by a current normal to layers, at 4 K.

In the present work, we consider the inverse effect. We assume that an external microwave is used to excite ferromagnetic resonance at a frequency $\omega/2\pi \simeq 1-50$ GHz in one ferromagnetic layer of a multilayer; we predict that this precession of the magnetization will generate a dc voltage across the multilayer. For sufficiently large precession amplitude, we find that V is of order $\hbar\omega/e \simeq 10\,\mu$V. Slonczewski has recently made a similar prediction.[6]

We consider [Fig. 1(a)] a magnetic multilayer similar to the one constituting the original SWASER.[1] The thick layer F_1 and the thin layer F_2 are ferromagnetic. The thin layer N and the thick layer N_2 are nonmagnetic. The precessing layer is assumed to be F_2. The magnetic spins in F_1 and F_2 are parallel in the absence of precession. They may be in the layer plane, or they may be pulled to the perpendicular direction by a static field. Since a constant value θ of the precession-cone angle is assumed in the present calculations, they apply only to the perpendicular case, strictly speaking. We attach electrodes to F_1 and N_2 to measure the voltage V.

The system of coordinates x,y,z [Fig. 1(a)] is such[1] that x is normal to the $N-F_2$ interface, and z is parallel to the magnetic spins in F_1. The origin of x is at the $N-F_2$ interface.

In the case of the SWASER, the configuration and chemical composition of the layers must not[3] possess mirror symmetry with respect to the median plane of the precessing layer, if the device is to function at all. We expect the same to be true of the present voltage generator, and for the same reasons.

In order to expose the multilayer to magnetic fields of microwave frequency, the multilayer may be enclosed in a waveguide. Alternatively, we may add a copper layer to the multilayer, insulated from other layers and connected to a coaxial cable; this has the advantage that resistors can be used for impedance matching. Similar coaxial-cable input has been used for other thin-film high-frequency magnetic devices.[7] Needed ac voltage in a 50 Ω cable is estimated by us at ≃0.15 V, to achieve a 30° precession cone angle in $Ni_{81}Fe_{19}$.

The skin effect in N_2 is not a problem, as long as the N_2

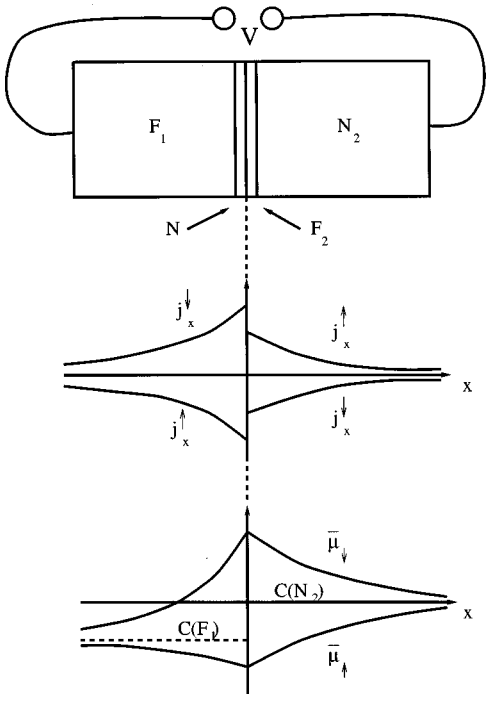

FIG. 1. (a) Multilayer with ferromagnetic layers F_1, F_2 and nonmagnetic layers N,N_2. (b) Spin-up and spin-down current densities $j_x^{\uparrow}, j_x^{\downarrow}$ in F_1 and N_2 as a function of coordinate x. (c) Average spin-up and spin-down electrochemical potentials $\overline{\mu}_{\uparrow}, \overline{\mu}_{\downarrow}$ in F_1 and N_2 as a function of coordinate x.

thickness is below the skin depth. The latter is estimated at $\simeq 2\ \mu$m, assuming 10 GHz and a nonmagnetic alloy of resistivity $\simeq 20\times 10^{-8}\,\Omega$m for N_2.

In principle, we can select which layer precesses, by exploiting possible differences in ferromagnetic resonance frequency. Instead of the layer configuration shown in Fig. 1(a) one could use the ''symmetric'' or the ''antisymmetric'' ones discussed in Ref. 3, or even the ''zero-current'' configuration.[3]

II. ELECTRON SPIN-FLIP PROCESSES IN LAYER F_2

The presence of interfaces between layers causes[1] a local enhancement of the isotropic s-d exchange interaction. Hence, we assume that this interaction is dominant in F_2 over other kinds of electron-magnon interactions such as anisotropic s-d exchange. Also, our numerical estimates indicate that it is dominant over spin-orbit interaction, as a source of electron spin flip in F_2, at the large precession amplitudes considered in the present paper.

We assume that each spin-wave mode of angular frequency ω' in F_2 contains an equilibrium number $[\exp(\hbar\omega'/k_BT)-1]^{-1}$ of quanta (magnons), except for one mode at the fixed angular frequency ω of an external ac magnetic field to which the multilayer is exposed. The latter mode contains an average number n_m of magnons, with $n_m \geqslant [\exp(\hbar\omega/k_BT)-1]^{-1}$. We assume a precessing layer F_2 of small dimensions, typically $3\,\text{nm}\times 1\,\mu\text{m}\times 1\,\mu$m; this excludes the possibility of many spin-wave modes of the same frequency. We will see in Sec. V how n_m is related to the precession-cone angle θ of the spin wave.

We ignore any interaction between spin-wave modes arising from nonlinear effects at the large precession amplitude considered in the present paper. We introduce[1] the net rate $dn_{\uparrow\downarrow}/dt$ of electron spin flip in F_2, from up to down, caused by spin waves of angular frequency ω. Because of angular-momentum conservation for isotropic exchange, one magnon of energy $\hbar\omega$ is created or annihilated for every electron spin-flip event.[1] We write the usual lowest-order form for $dn_{\uparrow\downarrow}/dt$:

$$\frac{dn_{\uparrow\downarrow}}{dt}=\int_{-\infty}^{+\infty} d\epsilon_{\uparrow}\frac{D_N}{4}B_{\uparrow\downarrow}f_{\uparrow}(\epsilon_{\uparrow})[1-f_{\downarrow}(\epsilon_{\uparrow}+\hbar\omega)]n_m - \int_{-\infty}^{+\infty} d\epsilon_{\downarrow}\frac{D_N}{4}B_{\uparrow\downarrow}f_{\downarrow}(\epsilon_{\downarrow})[1-f_{\uparrow}(\epsilon_{\downarrow}-\hbar\omega)](n_m+1). \tag{1}$$

Here, D_N is the density of states of conduction electrons. It is estimated in layer N, because this is where most of the norm of the wavefunction is assumed to be,[1] when calculating $dn_{\uparrow\downarrow}/dt$. Also, $\epsilon_{\uparrow}$ and $\epsilon_{\downarrow}$ are[1] the energies of spin-up and spin-down electron states and $f_{\uparrow}$ and $f_{\downarrow}$ their occupation numbers. And $B_{\uparrow\downarrow}$ is some positive coefficient representing the intensity of magnon-electron coupling in the layer F_2, which is[2] a function of the thickness L_2^x of the layer. The factors $1-f_{\uparrow}$, $1-f_{\downarrow}$ take into account the exclusion principle. The term $+1$ in Eq. (1) corresponds to spontaneous emission of spin waves, which had been neglected in Refs. 1–3.

We assume[1] the values of $f_{\uparrow}$ and $f_{\downarrow}$ to be given by Fermi functions with different electrochemical potentials $\overline{\mu}_{\uparrow},\overline{\mu}_{\downarrow}$ having the dimension of an energy:

$$f_{\uparrow}(\epsilon_{\uparrow})=[\exp((\epsilon_{\uparrow}-\overline{\mu}_{\uparrow})/k_BT)+1]^{-1};$$

$$f_{\downarrow}(\epsilon_{\downarrow})=[\exp((\epsilon_{\downarrow}-\overline{\mu}_{\downarrow})/k_BT)+1]^{-1}.$$

Note that these electrochemical potentials are averaged over the whole Fermi surface.[3] They differ because the radii of the spin-up and spin-down Fermi surfaces are slightly contracted and expanded, respectively.

In Refs. 1 and 2, the electrochemical potentials $\mu_{\uparrow},\mu_{\downarrow}$ were averaged over only half $k_x>0$ of the Fermi surface. And the spin-up and spin-down Fermi surfaces were translated in momentum space, by different amounts, giving rise to a difference $\Delta\mu=\mu_{\uparrow}-\mu_{\downarrow}$. But that mechanism is inactive in the present case because the net current density j_x vanishes everywhere.

After neglecting the energy dependence of D_N and $B_{\uparrow\downarrow}$, we can evaluate the integrals in Eq. (1):

$$\frac{dn_{\uparrow\downarrow}}{dt}=\frac{D_N}{4}B_{\uparrow\downarrow}\left\{n_m-\left[\exp\left(\frac{\Delta\overline{\mu}(0)+\hbar\omega}{k_BT}\right)-1\right]^{-1}\right\}\times[\Delta\overline{\mu}(0)+\hbar\omega]. \tag{2}$$

Here, $\Delta\overline{\mu}(0)=\overline{\mu}_{\uparrow}(0)-\overline{\mu}_{\downarrow}(0)$, where the argument 0 refers to the fact that $\overline{\mu}_{\uparrow}$ and $\overline{\mu}_{\downarrow}$ are evaluated in F_2, i.e., at $x\simeq 0$. The term n_m corresponds to[1] absorption and stimulated emission of spin waves, and is consistent with Eq. (17) of Ref. 1. It is the basis of the SWASER, where a sufficiently large current crossing layer F_2 leads[3] to $\Delta\overline{\mu}+\hbar\omega<0$ (or alternatively[1,2] to $\Delta\mu+\hbar\omega<0$), and thus to intense stimulated emission of spin waves. On the other hand, the term $-\{\exp[(\Delta\overline{\mu}(0)+\hbar\omega)/k_BT]-1\}^{-1}$ corresponds to spontaneous emission, and is relatively small in the SWASER or in the present work. As expected, Eq. (2) predicts $dn_{\uparrow\downarrow}/dt=0$ if n_m has the value corresponding to thermal equilibrium at temperature T, and if $\Delta\overline{\mu}=0$.

So far, we have ignored the modes with angular frequency ω' different from ω. Our numerical estimates show that their contribution to $dn_{\uparrow\downarrow}/dt$ is one tenth of that of the ω mode, for fcc cobalt at 300 K, and much less at 77 K.

The theory of spin-wave emission by a tunneling junction between magnetic metals, exposed to a dc voltage, is somewhat similar.[8,9]

III. SPIN DIFFUSION IN LAYERS F_1 AND N_2

As we stated in the preceding section, in F_2 the dominant spin-flip process is electron-magnon scattering, because of the presence of intense spin waves. On the other hand, in F_1 and N_2, spin-flip scattering at solute atoms caused by spin-orbit interaction probably dominates.

Conservation of the total number of electrons in F_1 and N_2 gives,[10] for one-dimensional conduction

$$\frac{dj_x^{\uparrow}}{dx}=-\frac{dj_x^{\downarrow}}{dx}=\frac{\Delta\overline{\mu}}{\tau_{\text{sr}}ce}. \tag{3}$$

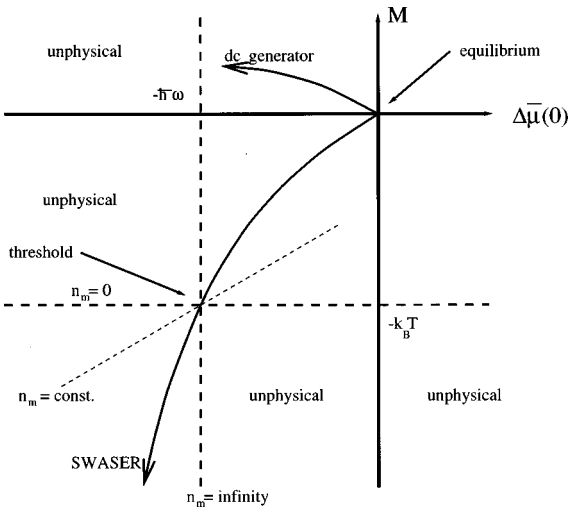

FIG. 2. The electrochemical potential difference $\Delta\overline{\mu}(0)$ is plotted in abscissa and the parameter M, which is proportional to incident microwave power, in ordinate. The two solid curves represent the trajectories of the SWASER and of the dc generator in this plane, as M is changed from zero.

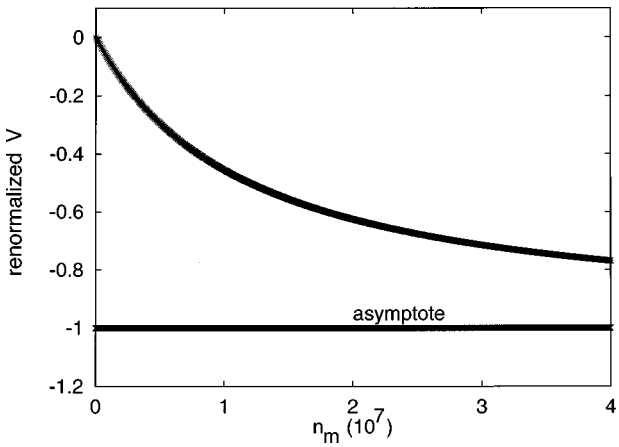

FIG. 3. Normalized values of dc voltage V across the multilayer, as a function of the number n_m of spin-wave quanta (magnons) in layer F_2, according to Eq. (12). The voltage V is expressed in units of $(\hbar\omega/2e)(\alpha_1-1)/(\alpha_1+1)$. Assumed parameter values are given in Sec. V.

We assume the multilayer to be in open circuit, so that the total current density j_x is zero everywhere:

$$j_x^{\uparrow}+j_x^{\downarrow}=j_x=0. \tag{4}$$

Here, c is the local electron density of states per unit volume and per spin, and τ_{sr} the conduction-electron spin-relaxation time. And $j_x^{\uparrow},j_x^{\downarrow}$ are the spin-up, spin-down current densities. We also write Ohm's and Fick's laws in combined form $j_x^{\uparrow}=(\sigma_{\uparrow}/e)d\overline{\mu}_{\uparrow}/dx$, $j_x^{\downarrow}=(\sigma_{\downarrow}/e)d\overline{\mu}_{\downarrow}/dx$. Combining these with Eq. (3), we obtain

$$\frac{\sigma_{\uparrow}}{e}\frac{d^2\overline{\mu}_{\uparrow}}{dx^2}=-\frac{\sigma_{\downarrow}}{e}\frac{d^2\overline{\mu}_{\downarrow}}{dx^2}=\frac{\Delta\overline{\mu}}{\tau_{sr}}ce. \tag{5}$$

From this, we also obtain Aronov's equation[11]

$$\frac{d^2\Delta\overline{\mu}}{dx^2}=\frac{\Delta\overline{\mu}}{l_{sr}^2};\quad l_{sr}=\left(\frac{\tau_{sr}}{ce^2(\sigma_{\uparrow}^{-1}+\sigma_{\downarrow}^{-1})}\right)^{1/2}. \tag{6}$$

Here, $\sigma_{\uparrow},\sigma_{\downarrow}$ are the spin-up, spin-down conductivities, and l_{sr} is the spin-diffusion length.

We solve Eqs. (3)–(6), together with Ohm's and Fick's laws, in F_1 and N_2, assuming these to be infinitely thick for the purpose of the present calculation. Solutions in each layer [Figs. 1(b), 1(c)] are of the general form

$$\overline{\mu}_{\uparrow}(x)=C+A_{\uparrow}e^{\pm x/l_{sr}},$$

$$\overline{\mu}_{\downarrow}(x)=C+A_{\downarrow}e^{\pm x/l_{sr}},$$

$$j_x^{\uparrow}(x)=\pm\Delta\overline{\mu}(0)e^{\pm x/l_{sr}}\frac{cel_{sr}}{\tau_{sr}},$$

$$j_x^{\downarrow}(x)=\mp\Delta\overline{\mu}(0)e^{\pm x/l_{sr}}\frac{cel_{sr}}{\tau_{sr}}, \tag{7}$$

where $C,A_{\uparrow},A_{\downarrow}$ are constants having different values in F_1 and N_2. The $\pm$ and $\mp$ signs before $\Delta\overline{\mu}(0)$ are correlated, to ensure $j_x=0$. For the same reason, the $\pm$ signs in the exponentials are also correlated.

Layers N and F_2 are assumed[3] to be much thinner than a local spin-diffusion length. Therefore, Ohm's and Fick's laws show that the variations of $\overline{\mu}_{\uparrow},\overline{\mu}_{\downarrow}$ across N and F_2 are small, and can be neglected. The existence of N and F_2 may be ignored for the present purpose, and we can talk[3] of an F_1-N_2 interface at $x\simeq 0$ [Fig. 1(a)]. While $\overline{\mu}_{\uparrow},\overline{\mu}_{\downarrow}$ are nearly continuous there [Fig. 1(c)] the existence of the intense spin-flip rate $dn_{\uparrow\downarrow}/dt$ in F_2 (Sec. II) implies nevertheless an electron transfer between the spin-up and spin-down currents, hence near discontinuities of $j_x^{\uparrow},j_x^{\downarrow}$ at $x\simeq 0$ [Fig. 1(b)]:

$$j_x^{\uparrow}(+0)-j_x^{\uparrow}(-0)=j_x^{\downarrow}(-0)-j_x^{\downarrow}(+0)=\frac{e}{L_yL_z}\frac{dn_{\uparrow\downarrow}}{dt}.$$

Here, $+0$ and -0 are slightly positive and negative values of x, corresponding to points just outside and on opposite sides of the very thin layer F_2. Also, L_y, L_z are the lateral sample dimensions. The multilayer being in an open circuit, we have also the condition $j_x^{\uparrow}(\pm\infty)=j_x^{\downarrow}(\pm\infty)=0$. We combine all these boundary conditions for $\overline{\mu}_{\uparrow},\overline{\mu}_{\downarrow},j_x^{\uparrow},j_x^{\downarrow}$ with Eqs. (7), and solve for $\Delta\overline{\mu}(0)$ and the voltage V across the multilayer. This voltage is defined by $-eV=C(N_2)-C(F_1)$ where $C(N_2),C(F_1)$ are the C values in F_1 and N_2.

$$V=\frac{\alpha_1-1}{\alpha_1+1}\frac{\Delta\overline{\mu}(0)}{2e}$$

$$\Delta\overline{\mu}(0)=-\frac{(dn_{\uparrow\downarrow}/dt)(e/L_yL_z)}{[el_{sr}(\sigma_{\uparrow}^{-1}+\sigma_{\downarrow}^{-1})]_{F1}^{-1}+[el_{sr}(\sigma_{\uparrow}^{-1}+\sigma_{\downarrow}^{-1})]_{N2}^{-1}}. \tag{8}$$

Here, the subscripts $F1,N2$ refer to the layers F_1, N_2. We have $dn_{\uparrow\downarrow}/dt>0, \Delta\overline{\mu}(0)<0, V<0$. Also, $\alpha_1 = \delta_\uparrow/\delta_\downarrow$ in F_1.

IV. STEADY STATE OF SPIN WAVES IN F_2

We consider a steady state for spin waves in F_2, with zero total dn_m/dt. There is an electron spin flip for each magnon created or annihilated in F_2 through s-d exchange (see Sec. II). Hence, the net rate dn_m/dt of the magnon creation caused by this process is equal to the net spin-flip rate $dn_{\uparrow\downarrow}/dt$, given by Eq. (2), with a change of sign. This contribution represents the first part of the total dn_m/dt in the following equation for the steady state:

$$0=\frac{dn_m}{dt}=-\frac{D_N}{4}B_{\uparrow\downarrow}\left\{\left[n_m-\left(\exp\left(\frac{\Delta\overline{\mu}(0)+\hbar\omega}{k_BT}\right)-1\right)^{-1}\right]\times[\Delta\overline{\mu}(0)+\hbar\omega]-M\right\}. \quad (9)$$

In addition, the microwave field of frequency $\omega/2\pi$ is acting on F_2 (Fig. 1), and creating magnons of the same frequency, as in ferromagnetic-resonance experiments. This rate of creation is represented in compact form by the second part M in Eq. (9). The variable $M\geqslant 0$ has the dimension of an energy.

We can solve Eq. (9) for n_m:

$$n_m=\left[\exp\left(\frac{\hbar\omega+\Delta\overline{\mu}(0)}{k_BT}\right)-1\right]^{-1}+\frac{M}{\hbar\omega+\Delta\overline{\mu}(0)}. \quad (10)$$

As expected, n_m in Eq. (10) is given by the usual Bose-Einstein formula in the special case of thermal equilibrium with $\Delta\overline{\mu}(0)=0$, $M=0$.

In the high-temperature limit $|\hbar\omega+\Delta\overline{\mu}(0)|\ll k_BT$, Eq. (10) reduces to

$$n_m\simeq\frac{k_BT+M}{\hbar\omega+\Delta\overline{\mu}(0)}. \quad (11)$$

If the dominant quantity ''pumping'' the SWASER happens to be $\Delta\overline{\mu}$ rather than $\Delta\mu$ (see Sec. II), then Eq. (11) applies even to a SWASER where the net current density j_x is not zero. This equation may be used to compare the SWASER to the present spin-wave driven dc generator. We show the $\Delta\overline{\mu}(0), M$ plane in Fig. 2. Since $n_m\geqslant 0$ by definition in Eq. (11), k_BT+M and $\hbar\omega+\Delta\overline{\mu}(0)$ must have the same sign for a physical state to exist. The region with $M<0$, $\Delta\overline{\mu}(0)<0$ corresponds to the SWASER, and the region with $M>0$, $\Delta\overline{\mu}(0)<0$ to the dc generator (Fig. 2). The origin corresponds to thermal equilibrium. The point $M=-k_BT$, $\Delta\overline{\mu}(0)=-\hbar\omega$ corresponds to the threshold for SWASER action. As shown by Eq. (11), the contours of constant n_M are straight lines passing through this threshold point. The solid curves are possible trajectories of a SWASER and of a dc generator in this plane as M is changed from zero.

V. CALCULATION OF VOLTAGE V

Considering the high-temperature limit $|\hbar\omega+\Delta\overline{\mu}(0)|\ll k_BT$, we substitute Eq. (2) into Eqs. (8) and obtain

$$V=\frac{\alpha_1-1}{\alpha_1+1}\frac{1}{2e}\frac{k_BT-n_m\hbar\omega}{(4L_yL_z/eD_NB_{\uparrow\downarrow})\{[el_{sr}(\sigma_\uparrow^{-1}+\sigma_\downarrow^{-1})]_{F1}^{-1}+[el_{sr}(\sigma_\uparrow^{-1}+\sigma_\downarrow^{-1})_{N2}^{-1}]\}+n_m}. \quad (12)$$

We estimate n_m from the precession-cone angle θ, for a layer F_2 of dimensions $L_y=L_z=1\ \mu$m, $L_2^x=3$ nm, made of fcc cobalt, by Eq. (18) of Ref. 1:

$$n_m=S_2(1-\cos\theta)n_2\simeq(S_2n_2\sin^2\theta)/2,$$

where S_2 is the magnitude of a localized atomic spin and n_2 the number of atoms in F_2. For $\theta=30°$, we find $n_m=3.1\times10^7$. Assuming $\omega/2\pi=10$ GHz, then $n_m\hbar\omega=1.3\times10^3$ eV. At $T=77$ K, then $k_BT\simeq0.66\times10^{-2}$ eV. Thus, the second term usually dominates, in the numerator of Eq. (12).

Now, we evaluate the denominator of Eq. (12). The magnon-electron parameter $B_{\uparrow\downarrow}$ may be estimated roughly by comparing our Eq. (9) to Eq. (19) of Ref. 1. We use $D_N/V_N=11.4\times10^{46}\,\mathrm{J^{-1}\,m^{-3}}$ as for copper,[1] $l_{sr}=44$ nm and $\sigma_\uparrow^{-1}=23\times10^{-8}\,\Omega$m, $\sigma_\downarrow^{-1}=48\times10^{-8}\,\Omega$m in both F_1 and N_2, as for cobalt nanowires[12] at 77 K. Then, the first term of the denominator is found to be 1.20×10^7, somewhat smaller than the maximum possible value $n_m=3.1\times10^7$ of the second term, quoted above. The exact value of $B_{\uparrow\downarrow}$ depends on the thickness of F_2; actually, both the F_2-N_2 and $N-F_2$ interfaces contribute[2,3] to $B_{\uparrow\downarrow}$.

We conclude that V approaches for large n_m the asymptotic value $V=-(\hbar\omega/2e)(\alpha_1-1)/(\alpha_1+1)$ given by these second terms in Eq. (12). For $\alpha_1\simeq2$, $\omega/2\pi=10$ GHz, this value is $V\simeq-6.9\,\mu$V. It is shown as a horizontal straight line in Fig. 3. The solid curve shows the dependence of V on n_m predicted by Eq. (12) for 77 K and the parameter values quoted in this section. This curve crosses the horizontal axis for $n_m\simeq k_BT/\hbar\omega\simeq161$, which is the n_m value for thermal equilibrium at 77 K.

As n_m increases, $\Delta\overline{\mu}(0)$ also approaches a fixed asymptotic value, equal to $-\hbar\omega$ [see the first Eq. (8)]. Then, Eq. (2) shows that Gilbert damping disappears gradually in F_2.

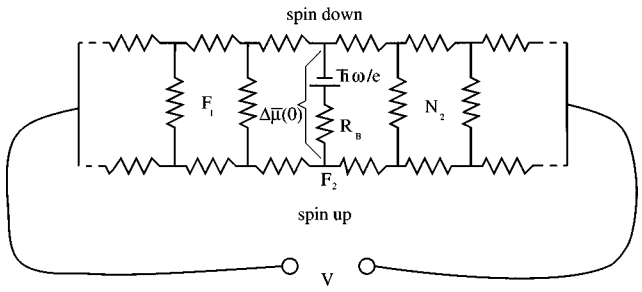

FIG. 4. Equivalent dc electrical circuit for the spin-wave driven dc generator considered in the present paper. Conduction in the spin-up and spin-down bands is represented by the lower and upper halves of the circuit, respectively. The current through the battery corresponds to the spin-flip rate $dn_{\uparrow\downarrow}/dt$ caused by spin waves in F_2. The currents through the vertical resistors on the left and right of the picture represent spin-orbit-induced spin-flip processes in F_1 and N_2, respectively.

VI. EQUIVALENT ELECTRICAL CIRCUIT

Electrical conduction and spin-flip processes in F_1 and N_2 [Eqs. (3)–(8)], together with spin-wave induced spin flip in F_2 [Eqs. (2)], may be represented by a dc equivalent circuit.

This circuit (Fig. 4) is somewhat similar to an unbalanced Wheatstone bridge. The fixed term $\hbar\omega$ at the end of Eq. (2) corresponds to the electromotive force $\hbar\omega/e$ of the battery which powers the bridge. It pumps electrons from the spin-up to the spin-down bands, represented by the lower and upper parts of the circuit, respectively. Also, $\Delta\overline{\mu}(0)$ at the end of Eq. (2) is represented by the actual voltage $\Delta\overline{\mu}(0)/e$ between the ends of the battery link in Fig. 4. The spin-flip rate $dn_{\uparrow\downarrow}/dt$ in Eq. (2) is represented by the current through the battery link, and $n_m-\{\exp[(\Delta\overline{\mu}(0)+\hbar\omega)/k_BT]-1\}^{-1}$ in Eq. (2) is represented by the reciprocal of the internal resistance R_B of the battery.

The left-hand part of the circuit (Fig. 4) represents conduction in layer F_1, and the right-hand part conduction in N_2. The value of each horizontal resistor is proportional to the local value of the resistivities $\sigma_\uparrow^{-1}$ or $\sigma_\downarrow^{-1}$. The bridge is unbalanced if $\alpha_1\neq 1$. On the other hand, the currents through the vertical resistors represent spin-orbit-induced spin-flip processes in F_1 or N_2, described by Eq. (3). The resistance of each vertical resistor is proportional to the local value of τ_{sr}.

The bridge-output wires at the extreme left and right of Fig. 4 represent the two leads connected to the external surfaces of F_1 and N_2 [Fig. 1(a)], to measure in open circuit the dc voltage across the multilayer.

This equivalent circuit may be used to better understand our results of Eq. (12) and Fig. 3 for the voltage V. As n_m increases from its equilibrium value, the internal resistance R_B of the battery decreases from infinity in the equivalent circuit. Of course, this has the effect of increasing the actual voltage $\Delta\overline{\mu}(0)/e$ across the battery link, from zero toward a value close to the full electromotive force $\hbar\omega/e$ of the battery. In turn, due to the bridge imbalance, the bridge output voltage V (Fig. 4) is some fraction $(1/2)(\alpha_1-1)/(\alpha_1+1)$ of that actual battery voltage. This agrees with the predictions of Eqs. (8) and (12), and with Fig. 3.

VII. STABILITY OF SPIN PRECESSION

Spin precession during ferromagnetic resonance is subject to several kinds of instabilities, especially at high values of θ where the equations of motion become nonlinear. One of them, called foldover, arises because there are three possible steady-state values of θ for given field and microwave power. Nevertheless, analytical[13] and numerical[14] calculations indicate that the precession can be stable even at θ values as high as 50°; one example is a flat disk of garnet with field normal to the disk plane, and with microwave frequency slightly below the small-signal resonance frequency. Experiments[15] are in fair agreement with the predictions of this theory. This suggests that a steady spin precession with $\theta\simeq 30°$, as often assumed in the present paper, is not unreasonable.

VIII. CONCLUSIONS AND FINAL REMARKS

The main result of the present paper is found in Eq. (12) and Fig. 3, which describe the dependence of the dc voltage V across the multilayer on the number n_m of spin-wave quanta (magnons) in layer F_2. The latter spin waves are excited by microwave power represented by the parameter M in Eq. (11). We find that V approaches a fixed value $-(\hbar\omega/2e)(\alpha_1-1)/(\alpha_1+1)\simeq -10\,\mu$V for large values of n_m. Here, α_1 is the ratio of spin-up and spin-down conductivities in the magnetic layer F_1, and ω the angular frequency of spin waves in F_2.

In the case of the SWASER, where spin precession is driven[1] by a dc current, an extra dc voltage across the multilayer, associated with the precession, was also predicted[1] to exist. This voltage was also of order $\hbar\omega/e$, but was of the opposite sign to the present voltage V because the sense of energy flow was from the current to the precessing spins, rather than the other sense.

A dc voltage $\hbar\omega/e$ is also predicted[16] across a magnetic domain wall precessing at an angular rate ω. The dependence of voltage on current is characterized[17] by steps of value $\hbar\omega/e$ for a superconducting tunneling junction exposed to a microwave of angular frequency ω. Finally, the same formula gives correctly the order of magnitude of the voltage across a photovoltaic cell, even though ω is much larger.

As in the case of a superconducting-junction voltage standard,[18] the measured voltage may be amplified by connecting several multilayers in series. Another way to increase V is to increase ω.

Juretschke and his collaborators[19] have observed dc voltages up to 600 μV in a ferromagnetic film exposed to an intense microwave. These voltages were related to the Hall effect and to the anisotropic magnetoresistance in the film. The voltage was measured between two points on a line parallel to the film plane. On the other hand, in the present paper the two points are on a line normal to the film plane. Moreover, the electric field (voltage per unit length) is larger in our case by a factor $\simeq 10^4$.

[1] L. Berger, Phys. Rev. B **54**, 9353 (1996).
[2] L. Berger, J. Appl. Phys. **81**, 4880 (1997).
[3] L. Berger, IEEE Trans. Magn. **34**, 3837 (1998).
[4] J. C. Slonczewski, J. Magn. Magn. Mater. **159**, L1 (1996).
[5] M. Tsoi, A. G. M. Jansen, J. Bass, W.-C. Chiang, M. Seck, V. Tsoi, and P. Wyder, Phys. Rev. Lett. **80**, 4281 (1998).
[6] J. C. Slonczewski (private communication).
[7] M. Senda and Y. Koshimoto, IEEE Trans. Magn. **33**, 3379 (1997).
[8] S. Zhang, P. M. Levy, A. C. Marley, and S. S. P. Parkin, Phys. Rev. Lett. **79**, 3744 (1997).
[9] W. A. Thompson, F. Holtzberg and S. Von Molnar, IBM J. Res. Dev. **14**, 279 (1970); J. A. Appelbaum and W. F. Brinkman, Phys. Rev. **183**, 553 (1969).
[10] T. Valet and A. Fert, Phys. Rev. B **48**, 7099 (1993).
[11] A. G. Aronov, JETP Lett. **24**, 32 (1976).
[12] L. Piraux, S. Dubois, and A. Fert, J. Magn. Magn. Mater. **159**, L287 (1996).
[13] D. J. Seagle, S. H. Charap, and J. O. Artman, J. Appl. Phys. **55**, 2578 (1984), see Fig. 3.
[14] J. O. Artman, S. H. Charap, and D. J. Seagle, IEEE Trans. Magn. **MAG-19**, 1814 (1983), see Figs. 6(a), 6(b).
[15] D. J. Seagle, J. O. Artman, and S. H. Charap, IEEE Trans. Magn. **MAG-21**, 1785 (1985), see Fig. 5.
[16] L. Berger, Phys. Rev. B **33**, 1572 (1986).
[17] A. H. Dayem and R. J. Martin, Phys. Rev. Lett. **8**, 246 (1962).
[18] R. L. Kautz, C. A. Hamilton, and F. L. Lloyd, IEEE Trans. Magn. **23**, 883 (1987).
[19] W. G. Egan and H. J. Juretschke, J. Appl. Phys. **34**, 1477 (1963); W. M. Moller and H. J. Juretschke, Phys. Rev. B **2**, 2651 (1970).